THE JOURNAL OF PHYSICAL CHEMISTRY C

Article

pubs.acs.org/JPCC

Electronic Structure and Transition Energies in Polymer–Fullerene Bulk Heterojunctions

Robert A. Street,*[,†] Steven A. Hawks,[§] Petr P. Khlyabich,[⊥] Gang Li,[§] Benjamin J. Schwartz,[‡] Barry C. Thompson,[⊥] and Yang Yang[§]

[†]Palo Alto Research Center, Palo Alto, California 94304, United States

[§]Department of Materials Science and Engineering, University of California, Los Angeles, Los Angeles, California 90095, United States

[‡]Department of Chemistry and Biochemistry, University of California, Los Angeles, Los Angeles, California 90095, United States

[⊥]Department of Chemistry and Loker Hydrocarbon Research Institute, University of Southern California, Los Angeles, California 90089, United States

Supporting Information

ABSTRACT: Photocurrent spectroscopy is used to measure both the charge transfer and exciton optical absorption spectra of various bulk heterojunction organic solar cells. The energy difference between the polymer HOMO energy and the fullerene LUMO energy is obtained from the spectra, along with the disorder energy. Combining information from cells with several different polymers and fullerenes allows measurements of the energy differences between HOMO or LUMO energies for about 10 different polymers and fullerenes, with an estimated uncertainty of 50 meV. Heterojunction band offsets are obtained for the various cells, distinguishing between the excitonic and the single-carrier band offsets. The cell open-circuit voltage is shown to be closely correlated with the interface band gap. The exciton disorder energy is directly correlated to the band-tail disorder and we also consider the effects of exciton thermalization on the charge generation mechanism. The data indicate that an energy offset between the polymer exciton and the charge transfer ground state below about 0.25 eV adversely affects the cell performance, while a HOMO band offset below about 0.2–0.3 eV also degrades cell performance but by a different mechanism.

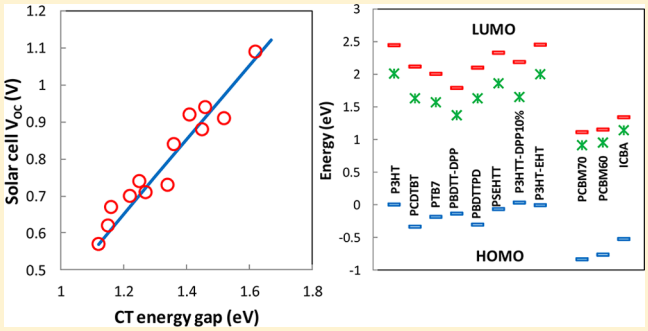

1. INTRODUCTION

Many organic semiconductors (OSC) have been developed as absorber materials for organic solar cells, which are typically paired with various fullerene derivatives to make bulk heterojunction (BHJ) active layers.[1] Solar cell efficiency has increased as a result of the new materials and device designs, but is still well below the theoretical limit.[2] The mechanisms that limit the cell efficiency are fairly well understood, and include the energy losses associated with exciton dissociation at the BHJ interface, optical absorption losses by nonoptimal absorber band gaps, and recombination losses by various possible mechanisms. The characteristics of these BHJ cells are largely determined by their electronic structure, in particular the relative highest occupied molecular orbital (HOMO) and lowest unoccupied molecular orbital (LUMO) levels, the exciton and charge transfer state energies, and the disorder energy. Accurate energy levels are therefore needed to understand the minimum band offset that can split an exciton, the dissociation probability of the charge transfer (CT) state, and the role of disorder in exciton diffusion and recombination.

Measurements of the HOMO and LUMO energy levels and transition energies have been made ever since studies of OPV began, with cyclic voltammetry and photoemission spectroscopy being the most widely used methods. Unfortunately, even for a well-studied cell such as poly(3-hexylthiophene):phenyl-C_{61}-butyric acid methyl ester (P3HT:PCBM), the reported HOMO and LUMO levels vary widely. Figure 1a plots a variety of reported literature values and shows P3HT HOMO values differing by ~0.5 eV and PCBM LUMO values by even more.[3] Energy levels with an accuracy of 0.1 eV or better are essential to understand the band offsets and other properties of BHJ cells. Since the important mechanisms of solar cell operation primarily depend on energy differences, it is more important to have relative energy-level values comparing the polymer and fullerene rather than absolute ionization and electron affinity energies for each material. This study uses optical spectroscopy, including measurements of the CT absorption band, from a

Received: July 16, 2014
Revised: August 27, 2014
Published: September 3, 2014

dx.doi.org/10.1021/jp507097h | J. Phys. Chem. C 2014, 118, 21873–21883

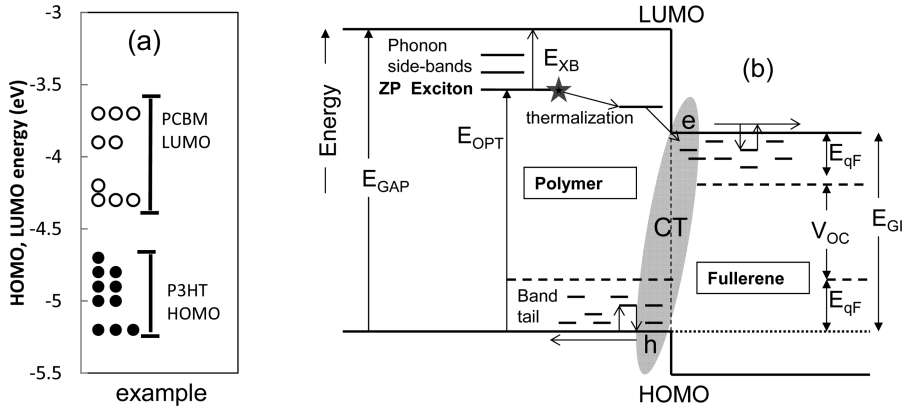

Figure 1. (a) A selection of literature values found by an Internet search for the P3HT HOMO and $PC_{60}BM$ LUMO energy, showing the large range of cited values. Each dot represents a cited value. (b) Schematic diagram of the bulk heterojunction structure showing the exciton and charge transfer (CT) excitations, as well as band-tail states and the electron and hole quasi-Fermi energies (E_{qF}). The zero-phonon exciton (ZP exciton) and the exciton sidebands are indicated.

range of polymers and fullerenes to obtain more accurate relative HOMO and LUMO levels, as well as exciton and charge-transfer transition energies. The interface band gap energy, the various heterojunction band offset energies, and the polymer disorder energy are obtained for a wide range of solar cell polymer and fullerene combinations. These energies are correlated with the cell performance to explore how they influence the charge generation and recombination mechanisms controlling cell efficiency.

2. METHODS AND MATERIALS

2.1. Background and Measurement Methodology.

The electronic processes involved in charge generation and recombination in the BHJ solar cell are illustrated in Figure 1b. Optical absorption creates excitons, primarily in the polymer but also in the fullerene. (For convenience we refer to the donor material in the BHJ structure as a polymer and the acceptor as a fullerene, as this is the case for all the samples studied, but the measurements equally apply to other organic material combinations.) The exciton absorption comprises a series of bands arising from the electron−phonon coupling, and the zero-phonon transition (ZP Exciton in Figure 1b) is the ground state exciton transition energy. The exciton may thermalize to a lower energy as it diffuses to the heterojunction interface since there is inevitably disorder in the exciton energy distribution. After reaching the domain interface, the exciton makes a transition to a CT state with some loss of energy, which is important to minimize for an efficient cell. The CT state dissociates into separate electrons and holes and these carriers interact with and occupy localized band-tail states arising from disorder in the polymer and fullerene. The polymer HOMO and fullerene LUMO have transport energies such that the majority of the conduction occurs near the transport energy.[4] The separation of these transport energies defines the effective interface band gap, E_{GI}.

When the cell is operated at open circuit, the electron and hole populations are in quasi-equilibrium with their respective transport energies, each defining a spatially flat quasi-Fermi energy E_{qF}, which together with E_{GI} determine the open circuit voltage:[2]

$$eV_{OC} = E_{GI} - E_{qFe} - E_{qFh} \quad (1)$$

The validity of eq 1 requires that the unilluminated built-in potential exceeds this value of V_{OC}. Inside the active layer, the electrons and holes are confined to the fullerene and polymer respectively by the heterojunction band offsets and the confinement suppresses electron−hole recombination by minimizing the overlap of the electron and hole wave functions. The details of the electronic structure, including the distribution of electronic states on both sides of the heterojunction interface, strongly influence all these processes.

Some studies of the BHJ electronic structure consider the CT state to have a discrete ground-state energy.[5] However, due to the presence of localized band-tail states arising from structural disorder at the molecular level,[6] and the additional longer-range conformational disorder of the BHJ internal interfaces, the CT state must represent an ensemble of ground-state configurations with a range of energies and perhaps with a range of dissociation rates. In addition there is a manifold of excited CT states giving a continuum of absorption transitions. Here we refer to the CT state to mean the immediate result of the exciton dissociation at the interface, including the ensemble of configurations and excited states. Many of the measurements described here are of the CT absorption, which reflects this ensemble of transition energies from the polymer HOMO to the fullerene LUMO bands.

The energy difference between the HOMO and LUMO transport energies, $E^{HOMO}_{polymer}$ and $E^{LUMO}_{fullerene}$, of polymer $P1$ and fullerene $F1$ defines the interface band gap $E_{GI}(P1,F1)$, as illustrated in Figure 1b:

$$E_{GI}(P1, F1) = E^{LUMO}_{fullerene}(F1) - E^{HOMO}_{polymer}(P1) \quad (2)$$

When two BHJ structures are compared that have the same fullerene $F1$ but two different polymers ($P2$ and $P3$) then

$$E^{HOMO}_{polymer}(P3) - E^{HOMO}_{polymer}(P2) = E_{GI}(P2, F1) - E_{GI}(P3, F1) \quad (3)$$

A corresponding expression applies to the LUMO levels of two different fullerenes with the same polymer. Equation 3 assumes that interfacial interactions (for example an interface dipole) that might modify the relative HOMO or LUMO levels are small or at least comparable in each case. Data analysis is presented in section 4.1 that indicates the assumption is valid for the devices that are measured. Therefore, the difference in the measured values of E_{GI}, when measured in two BHJ

dx.doi.org/10.1021/jp507097h | J. Phys. Chem. C 2014, 118, 21873−21883

structures that share the same polymer or fullerene, equals the difference in the HOMO transport energy between the two polymers or the LUMO transport energy of two fullerenes. Thus, the relative polymer HOMO and fullerene LUMO energy levels can be deduced from a sufficiently large set of polymer:fullerene combinations. Also, the relative energy levels of a pair of polymers or fullerenes can be obtained from different combinations of materials, which provides an estimate of the measurement uncertainty and a test of model assumptions for different material pairs.

The corresponding polymer LUMO and fullerene HOMO energies $E^{\mathrm{LUMO}}_{\mathrm{polymer}}$ and $E^{\mathrm{HOMO}}_{\mathrm{fullerene}}$ are found by adding or subtracting the appropriate band gap energy. It is important to differentiate clearly between the single carrier band gap E_{GAP} and the optical band gap E_{OPT} (see Figure 1b). E_{OPT} is measured by the onset of strong optical absorption and we define it to be the peak energy of the zero-phonon exciton transition. The single-carrier band gap is defined as the separation of the HOMO and LUMO transport energies for well-separated mobile holes and electrons, and is higher in energy than the optical gap by the exciton binding energy E_{XB}, this being the energy to dissociate electrons and holes within the polymer or fullerene. Hence for polymer $P1$ and fullerene $F1$

$$E^{\mathrm{LUMO}}_{\mathrm{polymer}} = E^{\mathrm{HOMO}}_{\mathrm{polymer}} + E_{\mathrm{OPT}}(P1) + E_{\mathrm{XB}}(P1)$$

$$E^{\mathrm{HOMO}}_{\mathrm{fullerene}} = E^{\mathrm{HOMO}}_{\mathrm{fullerene}} - [E_{\mathrm{OPT}}(F1) + E_{\mathrm{XB}}(F2)] \quad (4)$$

No measurements so far have unambiguously indentified the single-carrier polymer or fullerene band gap from optical absorption because it is hidden by the strong exciton absorption, but values obtained from photoemission spectroscopy have been reported.[7] The exciton energy is of primary interest for the optical absorption and exciton dissociation, but the single-carrier HOMO and LUMO are the relevant energies for electron and hole transport and recombination.

The exciton binding energy comprises two components, the Coulomb binding energy of the unrelaxed exciton E_{XC} and the reorganization energy E_{XR} arising from the electron−phonon coupling that adds to the binding energy, as illustrated in Figure 2.

$$E_{\mathrm{XB}} = E_{\mathrm{XC}} + E_{\mathrm{XR}} \quad (5)$$

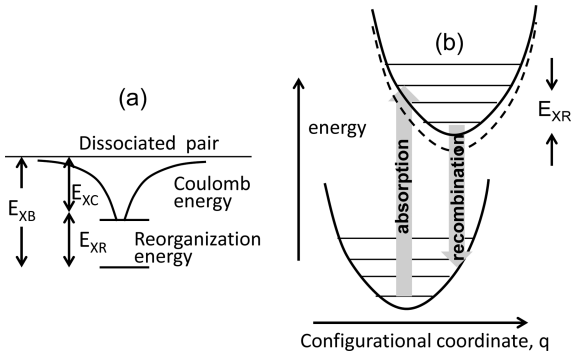

Figure 2. (a) Schematic illustration of the Coulomb and reorganization energy components of the exciton binding energy. (b) Configurational coordinate diagram illustrating the optical absorption and recombination transitions with a significant electron−phonon coupling. The dashed line illustrates the disorder broadening of the exciton energy.

It is well established that conjugated polymers exhibit multiple exciton absorption peaks reflecting phonon sidebands that arise from the structural relaxation and electron−phonon coupling.[8] The reorganization energy is described by a configurational coordinate diagram as shown in Figure 2b, which also illustrates the vibronic levels corresponding to the sidebands in the exciton absorption.[9,10] The general procedure to identify both the zero-phonon exciton energy and the reorganization energy is well established and is based on the relative intensities of the exciton absorption $I(N)$ (N = 0, 1, 2, etc.) of the phonon sidebands, given in terms of the Huang−Rhys (HR) coupling strength S:[11]

$$I(N) = S^N e^{-S}/N! \quad (6)$$

The reorganization energy is $E_{\mathrm{XR}} = S\hbar\omega_0$, where $\hbar\omega_0$ is the phonon energy that dominates the electron−phonon coupling. The exciton couples primarily to the 0.17−0.18 eV group of phonons in conjugated organic semiconductors, as several papers have reported.[8,12] These are phonon modes of the conjugated rings that comprise the polymer backbone (e.g., C═C stretching modes),[13] and they dominate the phonon coupling because the conjugated rings are the origin of the π-orbitals forming the exciton and hole wave functions. Coupling to the higher energy C−H modes is not observed because these bonds do not contribute to the π-orbitals. The absorption peak intensities in eq 6 are independent of temperature when $kT \ll \hbar\omega_0$, which applies well to the BHJ structures at room temperature since $\hbar\omega_0$ is approximately $7kT$. Possible corrections to the HR model are discussed further below.

2.2. Materials and CT Spectroscopy Measurements. Data for 13 bulk heterojunction solar cells with different polymer:fullerene combinations are reported, involving 7 different polymers and 3 fullerenes. A total of about 20 different samples were measured including the same combination made in different laboratories. The cells were fabricated in different laboratories by different groups and their fabrication and general properties are described elsewhere (see references for the materials below and Table 1). In addition some data were taken from the literature. The materials are the following: P3HT, poly(3-hexylthiophene);[14] PCDTBT, poly[carbazole-dithienyl-benzothiadiazole);[15,16] PTB7, poly(thieno[3,4-*b*]-thiophene/benzodithiophene);[17] PBDTT-DPP, poly{di-(ethylhexylthienyl)benzodithiophene-*alt*-5-dibutyloctyl-bis(5-bromothiophen-2-yl)pyrrolo pyrrole-dione};[18] P3HTT-DPP10%, poly(3-hexylthiophene-thiophene-diketopyrrolopyrrole);[19] P3HT-EHT, poly(3-hexylthiophene$_{75}$-*co*-3-(2-ethylhexyl)thiophene$_{25}$);[18] PSEHTT, poly[(bis(2-ethylhexyl)-dithienosilole)diyl-*alt*-(bis((2-ethylhexyl)thiophen-2-yl)-thiazolo thiazole)];[20] PBDTTPD, poly(di(2-ethylhexyloxy)-benzodithiophene-*co*-octylthienopyrrole-dione);[21] PC$_{60(70)}$BM, phenyl-C$_{61(70)}$-butyric acid methyl ester;[22] and ICBA, indene-C$_{60}$ bisadduct

Optical measurements using photocurrent spectroscopy were used to measure E_{GI}, E_{OPT}, and E_{XB}. The photocurrent spectral response (PSR) technique measures the optical absorption of transitions that generate photocurrent in the BHJ structure.[23] The technique is sufficiently sensitive to measure much lower absorption than standard optical absorption techniques and reveals the CT absorption at energies below the bulk exciton absorption. The measurement technique is described elsewhere and is performed either in a modified FTIR spectrometer[24] or by a standard photoconductivity measurement system with lock-in amplifier.[23,25] All the measurements were made at room

dx.doi.org/10.1021/jp507097h | J. Phys. Chem. C 2014, 118, 21873−21883

temperature, and the maximum monochromatic illumination intensity is <1 mW/cm^2, so that no significant sample heating occurs. Other sensitive optical absorption measurements have confirmed that the PSR data indeed measure the CT optical absorption and hence that the internal quantum efficiency for charge generation is independent of energy.[26]

3. RESULTS

3.1. Charge Transfer Spectra. Figure 3 shows PSR measurements of three different P3HT:PCBM solar cells

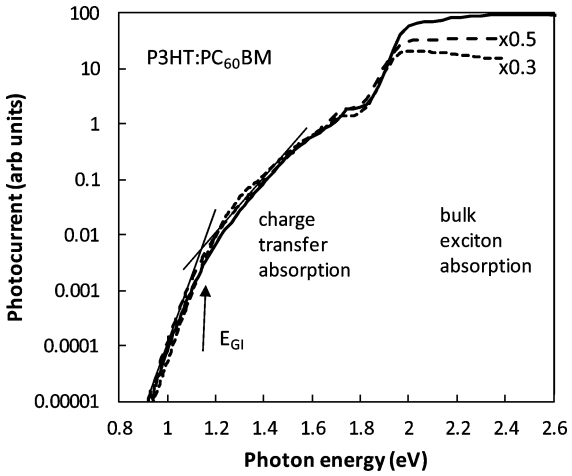

Figure 3. PSR spectra of P3HT:PCBM cells made by three different laboratories, scaled to match the CT absorption, with scaling parameters as indicated. Fine lines indicate the change of slope used to identify the interface band gap energy E_{GI}.

obtained from three different laboratories. The region above 1.9 eV corresponds to the bulk polymer exciton absorption and the lower energy portion of the spectrum is primarily from the CT absorption, with the fullerene exciton also observed at about 1.75 eV. The data have been scaled vertically to show that the CT absorption spectral absorption is almost identical in shape for the three samples, although its relative intensity compared to the exciton absorption differs by a factor of 3−4. The CT absorption arises from transitions at the molecular interfaces, so the different relative magnitude may reflect alternative nanometer-scale morphologies that have corresponding different effective internal areas of interface. The details of the CT absorption are related to the different active-layer morphology resulting from the cell fabrication, which has an impact on the polymer donor and fullerene acceptor domain size and interface area as well as on the electronic structure.[27] For these samples, the cell with the highest efficiency has the highest relative CT absorption and vice versa, as might plausibly be expected for devices with a larger interface internal area.

The PSR spectra of Figure 3 and other spectra shown in Figure 4 below do not reveal a unique marker of E_{GI} although inspection suggests that it is 1.1−1.2 eV for P3HT:PCBM, as we have indicated previously.[23,28] The fact that the intensity of the CT absorption relative to the excitons can vary for the same nominal material indicates that the location of E_{GI} must be found from the shape of the absorption band. Two models for the shape of the CT absorption have been proposed. Our preferred interpretation is that the shape of the CT absorption reflects the manifold of CT transitions arising from the density of states distributions of the polymer HOMO and fullerene LUMO, and that the effects of the electron−phonon coupling are small enough not to substantially change the spectral shape.[28] According to this view, the steeply decreasing absorption strength at the lowest energy arises from optical transitions in localized band-tail states. It is reasonable to suppose that the transport energy lies at the transition between the mobile band states and the exponential band-tail states in the HOMO or LUMO bands. Hence the change of slope of the CT absorption band provides a marker for E_{GI} that is easy to locate and consistent with the expected physical situation. This approach gives 1.15 eV for E_{GI} in P3HT:PCBM for the data in Figure 3. Our previous studies estimated a value of 1.2 eV for E_{GI} with use of a similar approach.[28]

The alternative model for the CT absorption proposes that the shape arises from a strong electron−phonon coupling, with a line-shape given by Marcus theory.[29] Analysis of the shape and the associated emission band leads to a CT energy of 1.14 eV for P3HT:PCBM. Earlier data by Vandewal et al.[30]

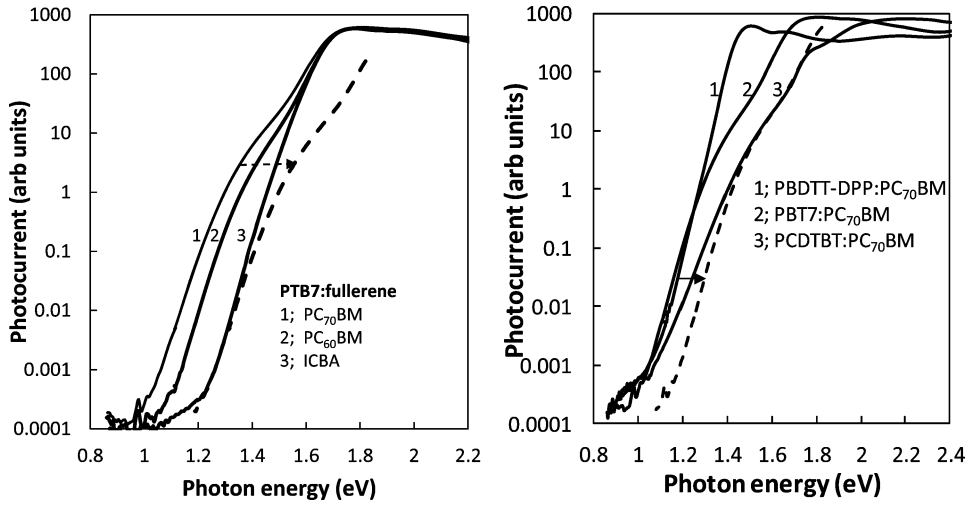

Figure 4. (a) Photocurrent spectral response (PSR) data for BHJ structures with one polymer (PBT7) and three different fullerenes, as indicated. The dashed line is the PBT7:PC$_{70}$BM data shifted to higher energy by 0.2 eV. (b) PSR data for three polymers and the same fullerene, as indicated. The dashed line is the PBT7:PC$_{70}$BM data shifted to higher energy.

dx.doi.org/10.1021/jp507097h | J. Phys. Chem. C 2014, 118, 21873−21883

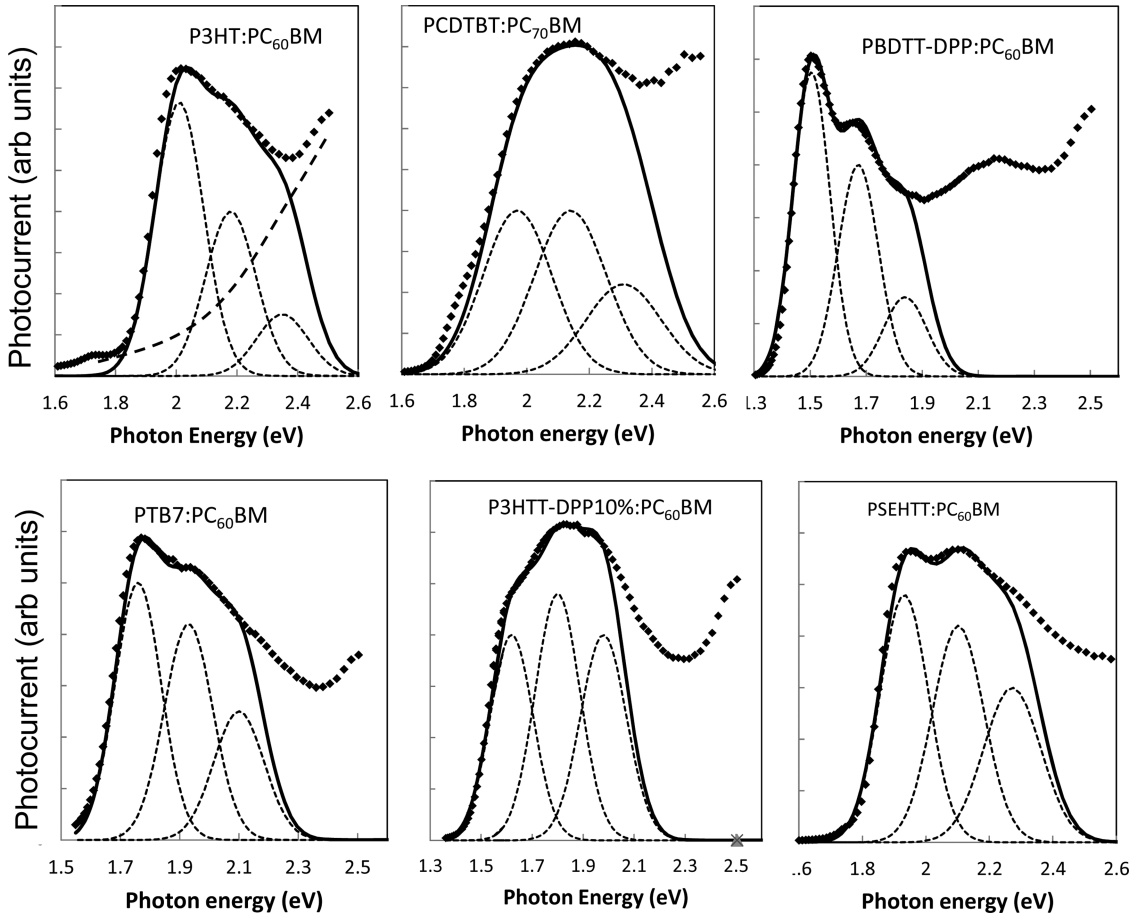

Figure 5. PSR spectra, plotted on a linear vertical scale, for six different polymer:fullerene structures as indicated. The solid lines are fits to the phonon-coupled series of exciton peaks as described in the text. The dashed line indicates the approximate background absorption of PCBM in P3HT:$PC_{60}BM$. The dotted lines are the individual peak fits, after correcting the intensities for the estimated background.

positioned E_{GI} at a significantly lower energy than more recent data.[29] Hence, although the two models make substantially different assumptions about the origin of the absorption, they result in almost exactly the same E_{GI} energy for P3HT:PCBM, and similar values are found in other cases where the two models can be compared. We therefore conclude that the change of slope in the CT absorption is a reliable marker for E_{GI}. The two alternative models are discussed further in the Supporting Information.

Figure 4a shows PSR measurements on BHJ cells that share the same PBT7 polymer and have different fullerenes, $PC_{70}BM$, $PC_{60}BM$, and ICBA. The spectrum above 1.7 eV is the same in each case because it reflects the polymer exciton absorption, while the signal below 1.7 eV is the CT absorption and shifts with the fullerene. The shift arises from the different fullerene LUMO levels, which change E_{GI} according to eq 2. To the extent that it can be seen, the CT absorption has the same shape in each case (the dashed line is the $PC_{70}BM$ data shifted by 0.2 eV to match the ICBA data). The higher energy region of the CT band is masked by the exciton absorption, but otherwise the shape is the same. Hence the relative shift of E_{GI} is easily obtained. The estimated value of E_{GI} is best obtained from the PTB7:$PC_{70}BM$ data since this shows the clearest CT absorption band, and we assign the position of E_{GI} in the same way as for P3HT:PCBM from the change of slope of the CT absorption. The position of E_{GI} for the other fullerenes is found from their relative shift.

This strategy of using the change of slope of the CT absorption where it is clearly visible and using the relative shift of the CT absorption for the cases when it is more hidden by the exciton absorption allows us to assign values of E_{GI} in all of the devices. In terms of the band-tail density of states interpretation of the low energy region of the PSR spectra, the similarity in shape between different fullerenes (Figure 4a) indicates that the polymer band-tail is broader than that of the fullerene and therefore determines the shape of the low energy PSR spectrum, in agreement with previous studies.[6]

Figure 4b shows an equivalent set of PSR spectra with the same $PC_{70}BM$ fullerene and different polymers. As expected, the exciton absorption region of the spectra is different as it reflects the different polymers. The CT absorption at lower energy also has a different shape and reflects the different HOMO levels of the polymer according to eq 2. Furthermore, unlike the data in Figure 3a, the slope of the low energy exponential from ~1 to 1.3 eV is also different. The density of states model for the CT absorption attributes the exponential slope to the localized band-tail states of the polymer, and hence it should be the same for samples with the same polymer but different for different polymers, as observed.

The dashed line in Figure 4b is the PBT7 data shifted by 0.14 eV. At PSR values above the change of slope, the shape of the spectrum is the same, but it differs at lower energy due to the different exponential slope. This comparison is consistent with the assignment of E_{GI} at the change of slope of the spectrum,

dx.doi.org/10.1021/jp507097h | J. Phys. Chem. C 2014, 118, 21873−21883

since we expect the band-like regions to be broadly similar, but the band-tails to be different for the various polymers.

The other polymer−fullerene combinations were analyzed by the same method. The uncertainty in locating the change of slope in the CT spectrum is about ±25 meV where the CT spectrum is observed over a wide energy range and increases when the CT spectrum is obscured by the bulk polymer absorption. As discussed further below, the difference in the fullerene LUMO energies measured in several different cell combinations differs by about ±30 meV, which also gives an estimate for the uncertainty from both measurement and other factors such as interface differences. If the transport energy is located at a different position in the CT absorption band then there will be a systematic shift in the energy values, but energy differences will be unchanged.

3.2. Exciton and Band Gap Energies. Figure 5 shows PSR data for a selection of cells plotted on a linear vertical scale, measuring the optical absorption in the region of the bulk exciton absorption bands, together with a fit to the exciton peaks in each of the data sets. Although the data could be obtained from conventional optical transmission measurements on films without electrodes, the PSR measurement provides exciton absorption data on the same sample and location within the sample as the CT absorption. The fit is based on three Gaussian bands separated by 0.17−0.18 eV, which is the known energy of the dominant phonon sideband. Three peaks are used for the fit because in most cases two peaks are clearly visible in the spectra and a third peak is less obviously present. In the case of PCDBTB:PCBM the peak structure is not visble, but for consistency we analyze the spectrum assuming the same phonon sideband progression. The fit parameters are the intensity of each peak and the Gaussian width.

The data show that the peak widths vary considerably between the different materials. In those cases where the peaks are quite sharp, the fit parameters are reasonably certain, but in those cases where the bands are broader and less clearly distinguished, the fit parameters are slightly less certain, because to some extent a different Gaussian width can be compensated by a change in the relative peak intensity. In addition there is background absorption, particularly from the fullerene that has a weak exciton absorption peak at about 1.7 eV and a steadily increasing absorption at higher energy. An estimate of the background absorption is shown by the dashed line in the P3HT:PCBM data of Figure 5. The peak intensities are corrected for the estimated background absorption and the corrected peaks are shown in Figure 5. For the purposes of this study, approximate peak intensities are sufficient, and the primary information is the relative strength of the first and second peak.

As described in section 2.1, the zero-phonon exciton energy ($N = 0$) is obtained by comparing the measured peak intensities with the predicted values to determine the sideband order of the peaks. The relative peak intensity according to eq 6 is plotted in Figure 6 for different values of S, up to 2.5. As S increases, the highest intensity peak is at a larger value of N and more sidebands contribute to the spectrum. The $N = 0$ peak has the highest intensity when S is <1 and the $N = 1$ peak has the highest intensity for $1 < S < 2$. S can therefore be identified from the intensity of the exciton peaks and gives the reorganization energy. Comparison of the model to the data indicates that S lies in a fairly narrow range of 0.7 to 1.4, and the reorganization energy $E_{XR} = S\hbar\omega_0$ is therefore 0.12−0.24 eV, reflecting moderate phonon coupling. The presence of the

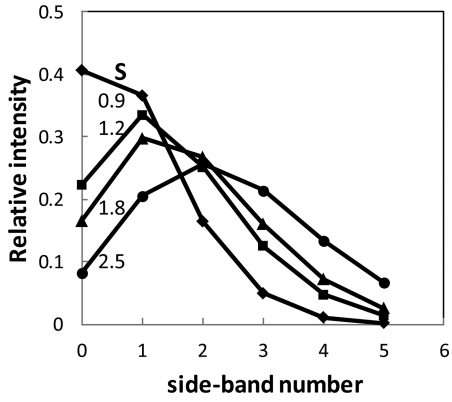

Figure 6. Plot of the predicted intensity of the zero-phonon ($N = 0$) line and phonon sidebands for different values of the Huang−Rhys factor S, according to eq 6.

background absorption from the fullerene absorption leads to a correction in the peak intensities of the vibronic series. The uncertain intensity of this background, along with the uncertainty of the other fitting parameters gives an uncertainty in S of ±0.2, based on estimated upper and lower limits of the background absorption. The resulting uncertainty in the value of E_{XR} ($=S\hbar\omega_0$) is only about 0.04 eV. The small value of S and the lack of significant absorption below the first absorption peak eliminate any ambiguity in the identification of the zero-phonon line.

It is possible that the polymer exciton absorption strengths deviate from the HR model. Brown et al. performed a detailed sideband analysis and suggested that there are two exciton series in P3HT with overlapping sidebands.[8] However, they also concluded that the lowest energy exciton is the zero-phonon transition. Spano showed that the HR intensities are modified by the molecular interactions in aggregated polymers.[31] For the case of an H-aggregate, the S values are overestimated by the HR model. However, at room temperature and when there is static disorder (see below), the effect is relatively small. Hence the error in using the simple model analysis should be small.

The unrelaxed exciton binding energy E_{XC} is difficult to obtain experimentally and thus has a much larger uncertainty than the reorganization energy. The value is not given by the PSR measurements or other optical absorption data and has been the subject of considerable debate, with values from zero to 0.5 eV or larger for the total exciton energy.[32] Based on published estimates, we choose a value of $E_{XC} = 0.3$ eV and combine this value with the reorganization energy to obtain the $E^{LUMO}_{polymer}$ values for the polymers. The total exciton binding energy obtained in this way is 0.45−0.55 eV and the LUMO transport energy of P3HT is 2.45 eV above the HOMO, which is consistent with photoemission spectroscopy measurement,[7] and provides some justification for the choice of $E_{XC} = 0.3$ eV. Note that some estimates of the LUMO energy are obtained by adding the optical band gap (i.e., the zero-phonon exciton energy) to the HOMO level, which by definition does not give the correct single-carrier LUMO energy.

The fullerene exciton energy is obtained by a similar approach. Literature data show that the fullerene exciton absorption near 1.7 eV is dominated by a single peak and that the photoluminescence spectrum has a peak at about the same energy and with only a weak phonon sideband.[20] We can therefore conclude that the main peak is the zero-phonon

dx.doi.org/10.1021/jp507097h | J. Phys. Chem. C 2014, 118, 21873−21883

Table 1. Parameters Obtained from Several BHJ Solar Cells Listed by Polymer and Fullerene[a]

	measured			derived		cell data		
materials	CT abs E_{GI} (eV)	polymer E_{OPT} (eV)	$E_{OPT} - E_{GI}$	$E^{HOMO}_{polymer} - E^{HOMO}_{fullerene}$	$E^{LUMO}_{polymer} - E^{LUMO}_{fullerene}$	V_{OC} (V)	fill factor	eff (%)
P3HT:$PC_{60}BM$	1.15	2.01	0.86	0.77	1.30	0.62	0.63	5
PCDTBT:$PC_{70}BM$	1.45	1.97	0.52	0.5	1.01	0.88	0.66	6.1
PBT7:$PC_{60}BM$	1.34	1.76	0.42	0.58	0.86	0.73	0.63	6.4
PTB7:$PC_{70}BM$	1.27	1.76	0.49	0.65	0.90	0.71	0.68	7.5
PTB7:ICBA	1.52	1.76	0.24	0.34	0.67	0.91	0.37	4.5
PBDTT-DPP:$PC_{70}BM$	1.25	1.51	0.26	0.7	0.68	0.74	0.66	
P3HT:ICBA	1.36	2.02	0.66	0.53	1.11	0.84	0.58	4
PBDTTPD:$PC_{60}BM$[b]	1.46	1.94	0.48	0.46	0.95	0.94	0.69	7.3
PBDTTPD:ICBA[b]	1.62	1.94	0.32	0.22	0.76	1.09	0.48	2.7
PSEHTT:$PC_{60}BM$	1.22	1.93	0.71	0.7	1.18	0.7	0.65	4.6
PSEHTT:ICBA	1.41	1.93	0.52	0.46	0.99	0.92	0.63	5.2
P3HTT-DPP10%:$PC_{60}BM$	1.12	1.62	0.5	0.8	1.04	0.57	0.62	5.1
P3HT-EHT:$PC_{60}BM$	1.16	2.01	0.85	0.76	1.30	0.67	0.59	3.2

[a] E_{GI} and E_{OPT} are measured and the other parameters are derived from these and from values in Table 2. V_{OC}, fill factor, and efficiency are obtained from cell measurements. [b] Measured values taken from literature data.[21]

energy and that the reorganization energy is small enough to be negligible. Again we do not know the exciton binding energy and estimate a value of 0.2 eV in recognition that the fullerene dielectric constant of roughly 4 is considerably larger than that of the polymers and hence the Coulomb component of the exciton binding energy should be smaller. This allows us to determine the fullerene $E^{HOMO}_{fullerene}$ energies.

4. DISCUSSION

4.1. Energy Level Summary. Table 1 gives the measured and analyzed energy levels and various other parameters for the set of BHJ cells. Table 2 shows the derived HOMO and LUMO levels, along with the optical gap (i.e., the zero-phonon exciton energy), the estimated exciton Coulomb binding energy, the Huang–Rhys factor S and the exciton reorganization energy for these same cells. Values for E_{GI}, the zero-phonon exciton energy, the energy difference between the exciton and E_{GI}, the measured V_{OC}, and the HOMO and LUMO band offsets are given for the listed BHJ structures, including some data from the literature. The HOMO energy of P3HT is defined as the zero of energy, and thus the data show the relative position of the HOMO and LUMO levels in other polymers and fullerenes. Band offsets for any combination of polymer and fullerene thus can be found from these values.

Table 2. Transport Energies of the Polymer and Fullerene HOMO and LUMO and Exciton Parameters for the Various Polymers and Fullerenes, Obtained As Explained in the Text[a]

polymer	$E^{HOMO}_{polymer}$ (eV)	$E^{LUMO}_{polymer}$ (eV)	E_{OPT} (eV)	E_{XC} (eV)	S	E_{XR} (eV)
P3HT	0	2.45	2.01	0.3	0.8	0.14
PCDTBT	−0.34	2.12	1.97	0.3	1.1	0.19
PTB7	−0.19	2.01	1.76	0.3	0.8	0.14
PBDTT-DPP	−0.14	1.79	1.51	0.3	0.7	0.12
PBDTTPD	−0.31	2.1	1.94	0.3	1	0.17
PSEHTT	−0.07	2.33	1.93	0.3	1	0.17
P3HTT-DPP10%	0.03	2.19	1.62	0.3	1.4	0.24
P3HT-EHT	−0.01	2.45	2.01	0.3	0.9	0.15
fullerene	$E^{HOMO}_{fullerene}$ (eV)	$E^{LUMO}_{fullerene}$ (eV)	E_{OPT} (eV)	E_{XC} (eV)	S	E_{XR} (eV)
$PC_{70}BM$	−0.84	1.11	1.75	0.2	0	0
$PC_{60}BM$	−0.77	1.15	1.72	0.2	0	0
ICBA	−0.53	1.34	1.67	0.2	0	0

[a] Values are referenced to the P3HT HOMO level.

Figure 7 displays the energy levels of the HOMO and LUMO transport energies and zero-phonon exciton energy relative to the HOMO energy for all the materials, referenced to the P3HT HOMO level. The polymer HOMO levels are generally consistent with other measurements even with the large variation in reported values. For example, the PCDTBT HOMO is reported to be −5.3 or −5.2 eV, and hence 0.2−0.4 eV lower that the typical values for P3HT (−4.9 to −5.2 eV), in agreement with our energy difference of ∼0.3 eV. The PTB7 HOMO level is reported to be −5.15 eV, and hence lies between P3HT and PCDTBT, also as we find here. However, whereas the range of literature values for the HOMO levels led to uncertainties in the energy differences ≥0.4 eV (see Figure 1a), the technique used here reduces the uncertainty to about 0.05 eV. In our comparison of the different fullerenes, we observe a range of values for the LUMO energy ($E^{LUMO}_{fullerene}$) difference for $PC_{70}BM$ and ICBA compared to $PC_{60}BM$. The different values are shown in Figure 7b for various polymer fullerene combinations. The energy difference for ICBA averages to 0.19 ± 0.03 eV, in good agreement with literature values of ∼0.2 eV.[33] The energy difference for $PC_{70}BM$ is about 0.04 ± 0.03 eV. The small variation in the values indicates that there are minimal differences arising from interface dipoles or other materials differences related to molecular packing or other variations in fullerene morphology in the systems that we measure.[34]

A consistency check on the various derived values is shown in Figure 8, which plots the 1-sun open circuit voltage V_{OC} reported for the various cells (see Table 1) as a function of the interface band gap E_{GI}, which is the relevant thermodynamic reference energy for the electron and hole. The data show that to a good approximation the energy difference, $D_E = E_{GI} - eV_{OC}$, is about 0.55 eV with small variation from cell to cell. It is well-known that the thermodynamic minimum value of D_E for an ideal solar cell with a band gap of 1.2−1.6 eV is ∼0.25 eV and only GaAs with D_E = 0.3 eV comes close to this limit.[35] Good silicon cells have D_E = 0.35−0.45 V and less efficient types of solar cells have larger values. High values of D_E arise

dx.doi.org/10.1021/jp507097h | J. Phys. Chem. C 2014, 118, 21873−21883

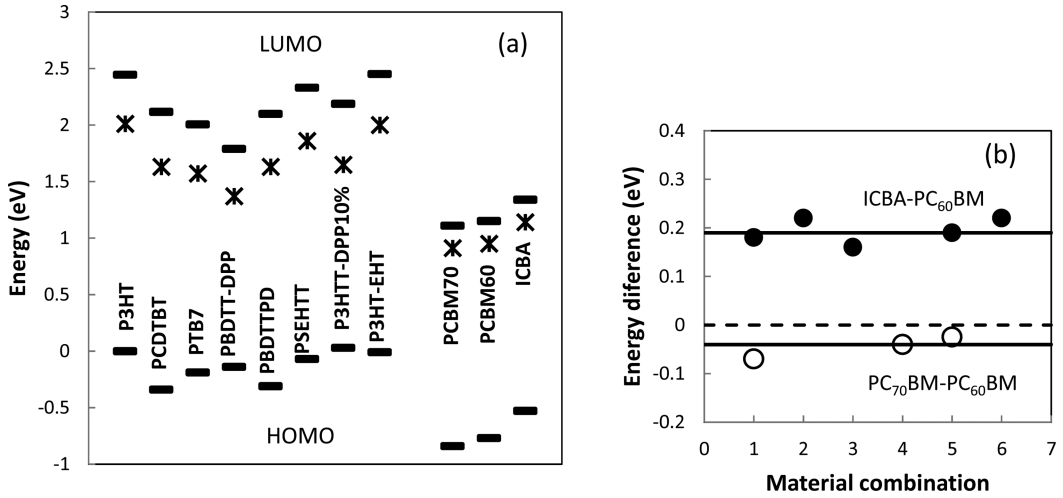

Figure 7. (a) HOMO and LUMO levels of the various polymers and fullerenes, relative to the P3HT HOMO energy. The star symbol shows the zero-phonon exciton energy relative to the HOMO level. (b) Energy level of ICBA and $PC_{70}BM$ relative to $PC_{60}BM$ measured on different material systems.

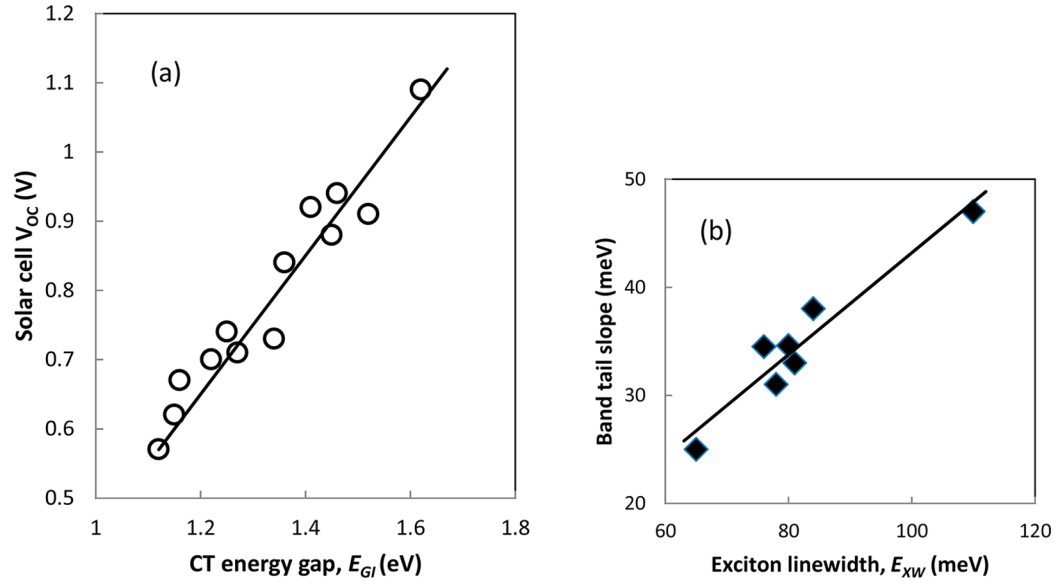

Figure 8. (a) Plot of the measured open circuit voltage V_{OC} and the CT band gap E_{GI} for the BHJ structures measured. The solid line reflects an energy difference $E_{GI} - eV_{OC} = 0.55$ eV. (b) Plot of the measured band-tail slope from the low energy exponential region of the PSR spectra, versus the bulk exciton line width obtained from the fit parameters for the data in Figure 5.

from recombination and reflect the splitting of the quasi-Fermi energies (qFE) and hence also reflect the magnitude of the carrier concentration at V_{OC}. Given the typical fill factor, efficiency, and other properties of present organic solar cells, D_E is unlikely to be less than 0.5 eV, but 0.55 eV is plausible and agrees with other estimates.[23] The 0.55 eV value for D_E is therefore evidence that the interface gap energies are correctly located. It has been suggested that values for $E_{GI} - eV_{OC}$ in organic solar cells may be as low as 0.3 eV,[36] which is too small given the typical fill factor, and probably results from inaccurate estimates for the HOMO and LUMO energies.

In principle, E_{GI} also can be obtained by extrapolating the linear regime of the temperature dependence of V_{OC} to $T = 0$ K, because $V_{OC} = E_{GI} - kT \ln(F)$ where F depends on the recombination mechanism. However, in the presence of disorder-induced band-tail states, the extrapolation of $V_{OC}(T)$ tends to slightly underestimate E_{GI}.[37] Additionally, accurate determination of E_{GI} from $V_{OC}(T)$ requires careful selection of the correct light-intesity regime for evaluating V_{OC}, since shunt resistance and built-in potential effects can mask the true quasi-Fermi level splitting in the bulk of the absorber.[38] Some measurements of P3HT:PCBM find extrapolated values of 1–1.1 eV,[26] consistent with our estimated E_{GI} of 1.15 eV.

4.2. Disorder and Thermalization in the Exciton and Band-Tail Absorption. The width (standard deviation) of the Gaussian fits to the zero-phonon optical absorption peak in Figure 5 gives a measure of the disorder in the exciton energy, while the slope of the low energy PSR spectrum gives a measure of the exponential band-tail disorder. Figure 8 compares these two values for the various polymers and shows a clear correlation. The material with the largest exciton line width and broadest band-tail slope is PCDTBT:PCBM while the smallest values arise from PBDTT-DPP:PCBM. PCDTBT is known to be amorphous,[15,16] while the other

dx.doi.org/10.1021/jp507097h | J. Phys. Chem. C 2014, 118, 21873–21883

polymers are semicrystalline, so the increased disorder is not surprising. PBDTT-DPP is one of the new polymers that exhibits high mobility associated with a more ordered material.[18] The exciton line may have thermal broadening, but the exciton widths are substantially larger than kT, and hence the largest component of the width is from disorder. The exciton width is about 10 times smaller in single crystal organic semiconductors at low temperature,[39] confirming that polymer/fullerene BHJ excitons are dominated by disorder.

It is natural to expect that the disorder in the electron states at the band edges will broaden both the exciton and the single carrier band-tail states. The observed broadening differs in magnitude by about a factor of 2, suggesting that the disorder affects the exciton and one-electron states differently. Although this may well be the case, the quantitative difference also may arise because the two measures of disorder—the Gaussian exciton width and the slope of the exponential band-tail—are not directly comparable. The correlation between the disorder in the polymer exciton and the band-tail CT absorption is further evidence that the CT absorption is dominated by the polymer HOMO band-tail state distribution rather than the fullerene LUMO states, which presumably have a narrower distribution of band-tail states.

In the presence of a distribution of states arising from disorder, optically excited excitons tend to thermalize into lower energy states as they diffuse. The thermalization energy is important because the energetics of exciton splitting at the fullerene interface depends on the thermalized exciton energy rather than the initial energy of the exciton absorption. Some solar cells listed in Table 1 have an energy difference between the exciton peak and the E_{GI} of only 0.2−0.3 eV, so that a thermalization energy of ∼0.1 eV makes a substantial difference to the energy released during exciton dissociation.

Studies of P3HT show that there is an energy shift of ∼0.18 eV between the zero-phonon exciton absorption and emission that is attributed to thermalization.[12] This energy shift is about twice the exciton line width E_{XW} and is consistent with expectations for thermalization over time constants typical for the emission. In general, an average exciton will lose $\sim E_{XW}$ in its first inelastic collision, but eventually thermalization stops at an energy where the energetic cost of thermal excitation to a higher energy is balanced by the reduced density of available lower energy states. However, excitons reach the BHJ interface rapidly, typically with picosecond time scale, and presumably after only a few scattering events. Thus, the thermalization energy could be substantially less than for the bulk emission band. Lacking any further experimental evidence, E_{XW} is a reasonable estimate for the thermalization energy, and hence in the range 60−110 meV.

4.3. Band Offsets. The energy loss ΔE_X when the exciton dissociates to form separate free mobile carriers is the difference between the zero-phonon polymer exciton energy and the interface band gap, $\Delta E_X = E_{OPT} - E_{GI}$, further reduced by a thermalization energy of order 0.1 eV, as discussed above. Table 1 shows that two of the cells (PBDTT-DPP:$PC_{70}BM$ and PBT7:ICBA) have a particularly small energy difference, being about ΔE_X = 0.25 eV. Interestingly, one of these (PBDTT-DPP:$PC_{70}BM$) has good cell performance with a high fill factor, but the cell performance of the other (PBT7:ICBA) is significantly reduced, compared to a PBT7 cell with a different fullerene for which $E_{OPT} - E_{GI}$ is larger. The fill factors for PBT7:$PC_{60}BM$ and PBT7:$PC_{70}BM$ are similar but the PBT7:ICBA fill factor is much smaller. Since ICBA gives an equally high fill factor as $PC_{60}BM$ in systems with other polymers including P3HT, the small energy offset may be responsible for the increased recombination (evident from the drop in fill factor in the case of PBT7), although morphological differences may also contribute.

The results from PBDTT-DPP also suggest that an energy difference ΔE_X of ∼0.2 eV may be close to the limit for efficient charge dissociation. The energy difference ΔE_X has a large influence on the cell efficiency, independent of any effect of recombination. According to eq 1 and Figure 8, $eV_{OC} = E_{OPT} - \Delta E_X - 0.55$. Hence, for the example of a polymer optical gap of 1.55 eV with other cell properties being unchanged, ΔE_X = 0.2 eV reduces V_{OC}, and hence the cell efficiency, by 20% and ΔE_X = 0.5 eV reduces the efficiency by 50% compared to ΔE_X = 0. It is therefore important to investigate systems with small energy differences to determine the ultimate low limit on the energy difference that still allows efficient charge separation.

The band offset between the two single carrier LUMO or HOMO energies is also important for the operation of the cell. This is the energy barrier that confines the mobile electrons to the fullerene and the holes to the polymer and determines the penetration of their wave functions into the other domain.[6] Table 1 and Figure 7 show that the band offsets for the LUMO levels are all quite large, from 0.5 eV to about 1.0 eV. This is a direct consequence of the requirement that the polymer exciton energy is larger than E_{GI}. The LUMO offset is essentially this energy difference plus the exciton binding energy of 0.4−0.5 eV. In contrast, Figure 7 and Table 1 show that the HOMO band offset can be much smaller and in two cases is only 0.2−0.3 eV. It is therefore of particular interest that in both cases of small HOMO band offset, the cell efficiency is low because of a reduced quantum efficiency and/or low fill factor. On the other hand the cell with a small ΔE_X energy offset but with high fill factor does not have a small HOMO band offset. This observation suggests that the small LUMO energy offset may not be the limiting factor, but instead a small HOMO offset limits the performance, possibly by enabling a recombination channel through the fullerene exciton, as others have proposed.[40] The problem is exacerbated in cells using ICBA since this material reduces the HOMO band offset, and the ICBA exciton is also at lower energy than the $PC_{60}BM$ exciton.

5. CONCLUSIONS

Photocurrent spectroscopy measurements on a wide range of BHJ cells allow improved measurement accuracy of the energy levels that are important for the electronic structure of organic BHJ solar cells, including the interface band gap, exciton zero-phonon energies, and energy band offsets. The open-circuit voltage of high fill factor cells is closely correlated to the interface band gap, the energy difference between the polymer HOMO and the fullerene LUMO. The energy difference between E_{GI} and V_{OC} is about 0.55 V and is consistent with expectations from solar cell theory. The disorder-induced broadening of the excitons and band-tail states are shown to be correlated. The results suggest that an energy difference between the zero-phonon exciton energy and the interface band gap of 0.25 eV may be close to the lower limit for practical solar cell operation. However, there the HOMO band offset can also limit the cell performance by opening an additional recombination channel, and the data indicate that this band offset needs to be larger than about 0.2−0.3 eV.

The results suggest some considerations for the design of better optimized cell materials, including several trade-offs that

need to be considered. Polymers with increased structural and electronic order will decrease the band-tail recombination due to a narrowing of the band-tail states, and may lose less low energy excitons when the exciton energy is close to E_{GI}. However, increased order also gives sharper absorption peaks and hence may reduce the overall absorption of the solar spectrum. Similarly, a large electron−phonon coupling reduces the absorption coefficient of the zero-phonon peak, but a very small phonon coupling gives a single sharp exciton peak and hence less absorption at higher energy. Careful optimization of the various parameters is needed, and any approach to the optimization of cell properties by designing new materials requires highly accurate energy level measurements. The measurements reported here have started along this road by improving the energy level accuracy compared to earlier studies, but the exciton binding energy still needs to be measured more accurately.

■ ASSOCIATED CONTENT

Supporting Information

Discussion on the mechanism of CT-state absorption, review of electron−phonon coupling theory, and application of the models to the CT absorption plus discussion of the CT-state emission spectrum. This material is available free of charge via the Internet at http://pubs.acs.org.

■ AUTHOR INFORMATION

Corresponding Author

*E-mail: street@parc.com. Tel 650-812-4165.

Notes

The authors declare no competing financial interests.

■ ACKNOWLEDGMENTS

P.P.K. and B.C.T. acknowledge partial support in the Center for Energy Nanoscience, an Energy Frontier Research Center funded by the U.S. Department of Energy, Office of Science, Office of Basic Energy Sciences, under Award DE-SC0001013. S.A.H acknowledges former support from an NSF IGERT: The Materials Creation Training Program (MCTP), DGE-0654431. S.A.H. and B.J.S acknowledge present support from the Molecularly Engineered Energy Materials (MEEM), an Energy Frontier Research Center funded by the U.S. Department of Energy, Office of Basic Energy Sciences under Award Number DE-SC0001342 and by the National Science foundation under grant NSF CHE-1112569. G.L. and Y.Y. acknowledge ONR, Grant No. N000141410648, and NSF, Grant No. DMR-1210893. The authors are grateful to T. Scholes (UCLA) for making the PSEHTT devices and S. Jenehke (U. Washington) for providing the PSEHTT polymer and to M. Cai and J. You for fabricating devices.

■ REFERENCES

(1) Brabec, C. J.; Gowrisanker, S.; Halls, J. J. M.; Laird, D.; Jia, S.; Williams, S. P. Polymer-Fullerene Bulk-Heterojunction Solar Cells. *Adv. Mater.* **2010**, *22*, 3839−3856.

(2) Dou, L.; You, J.; Hong, Z.; Xu, Z.; Li, G.; Street, R. A.; Yang, Y. 25th Anniversary Article: A Decade of Organic/Polymeric Photovoltaic Research. *Adv. Mater.* **2013**, *25*, 6642−6671.

(3) The values were obtained by an Internet search. They are not necessarily original sources and reflect the values cited by various researchers. Specific references are given in the Supporting Information.

(4) Kirchartz, T.; Pieters, B. E.; Kirkpatrick, J.; Rau, U.; Nelson, J. Recombination via Tail States in Polythiophene: Fullerene Solar Cells. *Phys. Rev. B* **2011**, *83*, 115209.

(5) Bredas, J. L.; Norton, J. E.; Cornil, J.; Coropceanu, V. Molecular Understanding of Organic Solar Cells: The Challenges. *Acc. Chem. Res.* **2009**, *42*, 1691−1699.

(6) Street, R. A. Localized State Distribution and Its Effect on Recombination in Organic Solar Cells. *Phys. Rev. B* **2011**, *84*, 75208.

(7) Deibel, C.; Mack, D.; Gorenflot, J.; Schöll, A.; Krause, S.; Reinert, F.; Rauh, D.; Dyakonov, V. Energetics of Excited States in the Conjugated Polymer poly(3-Hexylthiophene). *Phys. Rev. B* **2010**, *81*, 85202.

(8) Brown, P. J.; Thomas, D. S.; Köhler, A.; Wilson, J. S.; Kim, J.-S.; Ramsdale, C. M.; Sirringhaus, H.; Friend, R. H. Effect of Interchain Interactions on the Absorption and Emission of Poly(3-Hexylthiophene). *Phys. Rev. B* **2003**, *67*, 64203.

(9) Fowler, W. B. *Physics of Color Centers*; Academic Press: New York, NY, 1968.

(10) Hayes, W.; Stoneham, A. M. *Defects and Defect Processes in Nonmetallic Solids*; Courier Dover Publications: New York, NY, 2004.

(11) Huang, K.; Rhys, A. Theory of Light Absorption and Non-Radiative Transitions in F-Centres. *Proc. R. Soc. London, Ser. A* **1950**, *204*, 406−423.

(12) Spano, F. C.; Clark, J.; Silva, C.; Friend, R. H. Determining Exciton Coherence from the Photoluminescence Spectral Line Shape in poly(3-Hexylthiophene) Thin Films. *J. Chem. Phys.* **2009**, *130*, 074904.

(13) Wei, H.; Scudiero, L.; Eilers, H. Infrared and Photoelectron Spectroscopy Study of Vapor Phase Deposited Poly (3-Hexylthiophene). *Appl. Surf. Sci.* **2009**, *255*, 8593−8597.

(14) Chen, T. A.; Rieke, R. D. The First Regioregular Head-to-Tail poly(3-Hexylthiophene-2,5-Diyl) and a Regiorandom Isopolymer: Nickel versus Palladium Catalysis of 2(5)-Bromo-5(2)-(bromozincio)-3-Hexylthiophene Polymerization. *J. Am. Chem. Soc.* **1992**, *114*, 10087−10088.

(15) Blouin, N.; Michaud, A.; Leclerc, M. A Low-Bandgap Poly(2,7-Carbazole) Derivative for Use in High-Performance Solar Cells. *Adv. Mater.* **2007**, *19*, 2295−2300.

(16) Park, S. H.; Roy, A.; Beaupre, S.; Cho, S.; Coates, N.; Moon, J. S.; Moses, D.; Leclerc, M.; Lee, K.; Heeger, A. J. Bulk Heterojunction Solar Cells with Internal Quantum Efficiency Approaching 100%. *Nat. Photonics* **2009**, *3*, 297−303.

(17) Liang, Y.; Xu, Z.; Xia, J.; Tsai, S.-T.; Wu, Y.; Li, G.; Ray, C.; Yu, L. For the Bright Future-Bulk Heterojunction Polymer Solar Cells with Power Conversion Efficiency of 7.4%. *Adv. Mater.* **2010**, *22*, E135−E138.

(18) Dou, L.; You, J.; Yang, J.; Chen, C.-C.; He, Y.; Murase, S.; Moriarty, T.; Emery, K.; Li, G.; Yang, Y. Tandem Polymer Solar Cells Featuring a Spectrally Matched Low-Bandgap Polymer. *Nat. Photonics* **2012**, *6*, 180−185.

(19) Khlyabich, P. P.; Burkhart, B.; Thompson, B. C. Compositional Dependence of the Open-Circuit Voltage in Ternary Blend Bulk Heterojunction Solar Cells Based on Two Donor Polymers. *J. Am. Chem. Soc.* **2012**, *134*, 9074−9077.

(20) Subramaniyan, S.; Xin, H.; Kim, F. S.; Shoaee, S.; Durrant, J. R.; Jenekhe, S. A. Effects of Side Chains on Thiazolothiazole-Based Copolymer Semiconductors for High Performance Solar Cells. *Adv. Energy Mater.* **2011**, *1*, 854−860.

(21) Hoke, E. T.; Vandewal, K.; Bartelt, J. A.; Mateker, W. R.; Douglas, J. D.; Noriega, R.; Graham, K. R.; Fréchet, J. M. J.; Salleo, A.; McGehee, M. D. Recombination in Polymer:Fullerene Solar Cells with Open-Circuit Voltages Approaching and Exceeding 1.0 V. *Adv. Energy Mater.* **2012**, *3*, 220−230.

(22) Hummelen, J. C.; Knight, B. W.; LePeq, F.; Wudl, F.; Yao, J.; Wilkins, C. L. Preparation and Characterization of Fulleroid and Methanofullerene Derivatives. *J. Org. Chem.* **1995**, *60*, 532−538.

(23) Street, R. A.; Schoendorf, M.; Roy, A.; Lee, J. H. Interface State Recombination in Organic Solar Cells. *Phys. Rev. B* **2010**, *81*, 205307.

(24) Goris, L.; Poruba, A.; Hod'ákova, L.; Vaněček, M.; Haenen, K.; Nesládek, M.; Wagner, P.; Vanderzande, D.; De Schepper, L.; Manca, J. V. Observation of the Subgap Optical Absorption in Polymer-Fullerene Blend Solar Cells. *Appl. Phys. Lett.* **2006**, *88*, 052113.
(25) Bhattacharya, J.; Mayer, R. W.; Samiee, M.; Dalal, V. L. Photo-Induced Changes in Fundamental Properties of Organic Solar Cells. *Appl. Phys. Lett.* **2012**, *100*, 193501.
(26) Lee, J.; Vandewal, K.; Yost, S. R.; Bahlke, M. E.; Goris, L.; Baldo, M. A.; Manca, J. V.; Van Voorhis, T. Charge Transfer State Versus Hot Exciton Dissociation in Polymer-Fullerene Blended Solar Cells. *J. Am. Chem. Soc.* **2010**, *132*, 11878−11880.
(27) Youngkyoo, K.; Cook, S.; Tuladhar, S. M.; Choulis, S. A.; Nelson, J.; Durrant, J. R.; Bradley, D. D. C.; Giles, M.; McCulloch, I.; Chang-sik, H.; et al. A Strong Regioregularity Effect in Self-Organizing Conjugated Polymer Films and High-Efficiency Polythiophene:fullerene Solar Cells. *Nat. Mater.* **2006**, *5*, 197−203.
(28) Street, R. A.; Song, K. W.; Northrup, J. E.; Cowan, S. Photoconductivity Measurements of the Electronic Structure of Organic Solar Cells. *Phys. Rev. B* **2011**, *83*, 165207.
(29) Vandewal, K.; Tvingstedt, K.; Gadisa, A.; Inganas, O.; Manca, J. V. Relating the Open-Circuit Voltage to Interface Molecular Properties of Donor:acceptor Bulk Heterojunction Solar Cells. *Phys. Rev. B* **2010**, *81*, 125204.
(30) Vandewal, K.; Gadisa, A.; Oosterbaan, W. D.; Bertho, S.; Banishoeib, F.; Van Severen, I.; Lutsen, L.; Cleij, T. J.; Vanderzande, D.; Manca, J. V. The Relation between Open-Circuit Voltage and the Onset of Photocurrent Generation by Charge-Transfer Absorption in Polymer: Fullerene Bulk Heterojunction Solar Cells. *Adv. Funct. Mater.* **2008**, *18*, 2064−2070.
(31) Spano, F. C. The Spectral Signatures of Frenkel Polarons in H- and J-Aggregates. *Acc. Chem. Res.* **2009**, *43*, 429−439.
(32) Alvarado, S. F.; Seidler, P. F.; Lidzey, D. G.; Bradley, D. D. C. Direct Determination of the Exciton Binding Energy of Conjugated Polymers Using a Scanning Tunneling Microscope. *Phys. Rev. Lett.* **1998**, *81*, 1082−1085.
(33) Xin, H.; Subramaniyan, S.; Kwon, T.-W.; Shoaee, S.; Durrant, J. R.; Jenekhe, S. A. Enhanced Open Circuit Voltage and Efficiency of Donor−Acceptor Copolymer Solar Cells by Using Indene-C60 Bisadduct. *Chem. Mater.* **2012**, *24*, 1995−2001.
(34) Miller, N. C.; Sweetnam, S.; Hoke, E. T.; Gysel, R.; Miller, C. E.; Bartelt, J. A.; Xie, X.; Toney, M. F.; McGehee, M. D. Molecular Packing and Solar Cell Performance in Blends of Polymers with a Bisadduct Fullerene. *Nano Lett.* **2012**, *12*, 1566−1570.
(35) Nayak, P. K.; Bisquert, J.; Cahen, D. Assessing Possibilities and Limits for Solar Cells. *Adv. Mater.* **2011**, *23*, 2870−2876.
(36) Scharber, M. C.; Wuhlbacher, D.; Koppe, M.; Denk, P.; Waldauf, C.; Heeger, A. J.; Brabec, C. L. Design Rules for Donors in Bulk-Heterojunction Solar Cells - Towards 10% Energy-Conversion Efficiency. *Adv. Mater.* **2006**, *18*, 789−794.
(37) Manor, A.; Katz, E. A. Open-Circuit Voltage of Organic Photovoltaics: Implications of the Generalized Einstein Relation for Disordered Semiconductors. *Sol. Energy Mater. Sol. Cells* **2012**, *97*, 132−138.
(38) Hawks, S. A.; Li, G.; Yang, Y.; Street, R. A. Band tail recombination in polymer-fullerene organic solar cells. *J. Appl. Phys.* **2014**, *116*, 074503.
(39) Raimondo, L.; Silvestri, L.; Borghesi, A.; Tavazzi, S. Exciton−Lattice Phonon Coupling in Organic Semiconductor Crystals beyond the Static Disorder. *J. Phys. Chem. C* **2013**, *117*, 26248−26254.
(40) Faist, M. A.; Kirchartz, T.; Gong, W.; Ashraf, R. S.; McCulloch, I.; de Mello, J. C.; Ekins-Daukes, N. J.; Bradley, D. D. C.; Nelson, J. Competition between the Charge Transfer State and the Singlet States of Donor or Acceptor Limiting the Efficiency in Polymer:Fullerene Solar Cells. *J. Am. Chem. Soc.* **2012**, *134*, 685−692.